ADCHEM 2006

International Symposium on Advanced Control of Chemical Processes
Gramado, Brazil – April 2-5, 2006

NON LINEAR OBSERVER FOR THE RECONSTRUCTION OF CRYSTAL SIZE DISTRIBUTIONS IN POLYMORPHIC CRYSTALLIZATION PROCESSES

Toufik Bakir [*,1] **Sami Othman** [*] **Gilles Fevotte** [*]
Hassan Hammouri [*]

[*] *LAGEP, UMR CNRS 5007/ CPE Université Claude Bernard Lyon 1, 43 bd du 11 Nov. 1918, 69622 Villeurbanne Cedex France*

Abstract: This paper deals with the problem of estimating CSD (Crystal Size Distributions) during polymorphic crystallization processes. The proposed approach is based on the high gain observer using the discretization of the PBE's (Population Balance Equations). First, in the growth phase, the monitoring of the nuclei production permits the estimation of the CSD using an adequate observer. In the dissolution of the metastable phase, the lack of on line sensors doesn't allow to synthesize a classical observer. However, the stability of the PDE allows to design an open loop observer. In fact, this stability is necessary to guarantee the convergence of the proposed observer. The performance of the given observer is discussed in the presence of noise measurements.

Keywords: Chemical industry, Observers, Partial differential equations, Finite difference method, Nonlinear systems.

1. INTRODUCTION

In biotechnology and pharmaceutical industries, polymorphism may occur for many products, which means that a given compound may exhibit several crystal structures. Such industrial products are obtained generally in a solid state through a batch crystallization process. Polymorphic structures exhibit different physical and chemical properties such as crystal morphology, solubility, and color, which affect the performance of the ingredients. Concerning drugs, and from a safety point of view, the polymorphic structure has to be controlled to keep the proper product performance. To do so, on line measurements have to be realized. The monitoring of crystallization processes has been object of number of publications. In (Ono *et al.*, 2004), Raman spectroscopy was used in order to measure polymorphic composition, a simulation of the process was also developed. In (Starbuck *et al.*, 2002) and (Caillet *et al.*, 2006), the aim was also the monitoring of different transitions using in-situ Raman spectroscopy. In the current work, is designed an asymptotic observer to estimate the CSD yield by polymorphism in crystallization process. The performances of this technique are discussed through simulation results. The stability of the PDE (partial differential equation) describing the PBE of the CSD is basically used, it justifies the possibility of the estimation of distribution without specific measurements (dissolution phase), this part will be developed below.

The paper is organized as follows, the polymorphism in batch crystallization is briefly described

[1] bakir@lagep.univ-lyon1.fr

(section 2). The principle of discretization of the PBEs (Population Balance Equations) is then exposed in section 3. Section 4 is devoted to the observer synthesis. In section 5, the estimation technique is validated through simulation.

2. MODEL DEVELOPMENT

Polymorphism in crystallization process can be defined as a set of N crystalline forms produced in the same stirred reactor. The dynamical model of such process is described by a set of population balances, a material balance relating the solute concentration and the different solid concentration of the crystalline forms, and an energy balance for all the components of the reactor. In the case of two crystalline forms, the following population balance approach is applied for both CSDs (crystal size distributions), it yields the following partial differential equations (PDEs):

$$\frac{\partial n_1(x_1,t)}{\partial t} + G_1(t)\frac{\partial n_1(x_1,t)}{\partial x_1} = 0 \qquad (1)$$

$$\frac{\partial n_2(x_2,t)}{\partial t} + G_2(t)\frac{\partial n_2(x_2,t)}{\partial x_2} = 0 \qquad (2)$$

$n_1(x_1,t)$ and $n_2(x_2,t)$ are the number population density function for the two crystal forms respectively (stable and metastable forms). each function represents the number of crystals of size x_1 or x_2 per unit volume of suspension and per unit of size. In equations (1) and (2), only nucleation and growth are be considered, agglomeration and breakage are not taken into account. The growth kinetics $G_1(t)$ and $G_2(t)$ are assumed to be size independent.
The solute concentration balance describing the mass transfer from the liquid to the solid phase is:

$$\frac{dV_t(t)C(t)}{dt} + \frac{dV_T C_{S1}(t)}{dt} + \frac{dV_T C_{S2}(t)}{dt} = 0 \qquad (3)$$

$C(t)$ represents the solute concentration, V_T is the suspension volume, variations of this volume, due to solute mass transfer can be neglected. $C_{S1}(t)$ and $C_{S2}(t)$ being the solid concentration of the two phases, they can be deduced from the crystal size distributions (CSDs) :

$$C_{S1}(t) = \frac{K_{V1}\rho_s}{M_s}\int_0^\infty x_1^3 n_1(x_1,t)dx_1 \qquad (4)$$

$$C_{S2}(t) = \frac{K_{V2}\rho_s}{M_s}\int_0^\infty x_2^3 n_2(x_2,t)dx_2 \qquad (5)$$

where K_{V1} and K_{V2} are the shape factors for the two forms (for sphere $K_V = \frac{\pi}{6}$), M_s is the molecular weight of solid of density ρ_s, and $V_t(t)$ is the solution volume (i.e. the continuous phase), which is calculated as :

$$V_t(t) = V_T(1 - \frac{M_s}{\rho_s}C_{ST}(t)) \qquad (6)$$

with :

$$C_{ST}(t) = C_{S1}(t) + C_{S2}(t) \qquad (7)$$

The crystallizer temperature is described by the energy balance :

$$\sum_{i=1}^{3} Cp_i n_i \frac{\partial T_{cr}}{\partial t} = -\triangle H_c V_T \frac{dC_{ST}}{dt} - UA(T_{cr} - T_j) \qquad (8)$$

where Cp_i and n_i represent respectively the molar heat capacities and the number of moles of the different components in the crystallizer. T_{cr} and T_j are respectively the crystallizer and jacket temperatures. $\triangle H_c$ is the crystallization enthalpy. U and A_c are respectively the overall heat transfer coefficient and contact surface through the jacket wall. The solubility, which refers to the solute concentration under saturated conditions, is assumed to obey Van't Hoff equation and is given by :

$$C_{sat1}(T) = A_1 \exp(\frac{-\Delta H_c}{RT}) \qquad (9)$$

$$C_{sat2}(T) = A_2 \exp(\frac{-\Delta H_c}{RT}) \qquad (10)$$

$C_{sat1}(T)$ and $C_{sat2}(T)$ represent respectively the solubility for stable and metastable form ($A_1 < A_2$), the absolute supersaturation ($C - C_{sat}$) is the driving force of the crystallization process. When this value is positive, the overall growth rate, including possible diffusive limitations, is assumed to be represented by the following model.

$$G_1(t) = K_{c1}\frac{M_s}{2\rho_s}\eta_1(C(t) - C_{sat1}(t))^g \qquad (11)$$

$$G_2(t) = K_{c2}\frac{M_s}{2\rho_s}\eta_2(C(t) - C_{sat2}(t))^g \qquad (12)$$

where K_{c1} and K_{c2} represent the kinetic growth rate coefficients, η_1 and η_2 represent the effectiveness factors. For example, for the first population, η_1 is the solution of the following equation :

$$\frac{K_{c1}}{K_{d1}}(C(t) - C_{sat1}(t))^{g-1}\eta_1 + \eta_1^{\frac{1}{g}} - 1 = 0 \qquad (13)$$

K_{d1} represents the mass transfer coefficient through diffusion which will be assumed to be the same for all crystal sizes. In the literature, values of exponent g were generally assumed to lie between 1 and 2, Analytical solution of equation (13) is available if g is equal to 1 or 2, a numerical solution can be considered in the other cases.

In the case of a negative supersaturation, the growth kinetic is replaced by a dissolution kinetic, it takes the following form :

$$D_1(t) = -K_{dis1}\frac{M_s}{2\rho_s}(C(t) - C_{sat1}(t))^g \qquad (14)$$

$$D_2(t) = -K_{dis2}\frac{M_s}{2\rho_s}(C(t) - C_{sat2}(t))^g \qquad (15)$$

In this case, g is assumed to be equal to 2. K_{dis1} and K_{dis1} are the dissolution coefficients for stable and metastable population. Concerning the two populations, the nucleation rate B is the result of two competitive nucleation mechanisms. Primary nucleation takes place in the absence of any crystal in the solution :

$$B_{11} = A_{11}\exp\left(\frac{B_{11}}{\ln^2(\frac{C(t)}{C_{sat1}(t)})}\right) \qquad (16)$$

$$B_{21} = A_{21}\exp\left(\frac{B_{21}}{\ln^2(\frac{C(t)}{C_{sat2}(t)})}\right) \qquad (17)$$

and secondary nucleation, which may occur at lower supersaturation level, is favored by the presence of solid in suspension (i.e. added in the crystallizer through seeding or generated through primary nucleation) :

$$B_{12} = A_{12}M_{T1}^i(C(t) - C_{sat1}(t))^j \qquad (18)$$

$$B_{22} = A_{22}M_{T2}^i(C(t) - C_{sat2}(t))^j \qquad (19)$$

A_{11}, A_{21}, B_{11} and B_{21} are the primary nucleation parameters, A_{12} and A_{22} are the secondary nucleation parameters, M_{T1} and M_{T2} are respectively the crystal mass of the stable and metastable crystal form in the solution. In the case of positive supersaturation, the boundary condition for equations (1) and (2) are usually set as follows :

$$n_1(x_1^*, t) = \frac{B_1(x_1^*)}{G_1(x_1^*)} \simeq \frac{B_1}{G_1} \qquad (20)$$

$$n_2(x_2^*, t) = \frac{B_2(x_2^*)}{G_2(x_2^*)} \simeq \frac{B_2}{G_2} \qquad (21)$$

Where only small crystal nuclei of critical size x_1^* and x_2^* are assumed to grow.

At first, clear solution is prepared, the two forms being undersaturated. The solution is cooled until nuclei of the metastable form are produced. The production of metastable nuclei yields a decrease of the solute concentration. The decrease of the temperature generates more supersaturation, and thus, a growth of the two forms. The process behavior for the metastable form changes when metastable concentration crosses the metastable solubility curve. Dissolution of this form begins, and the polymorphic fraction of the metastable form decreases. At the same time, the growth of stable form continues until the consumption of the solute concentration.

This description is done in order to analyze the observability of both forms. Concerning the stable form, the nuclei production guarantees the observability during all of the process. It is the case for the metastable form until the behavior changes

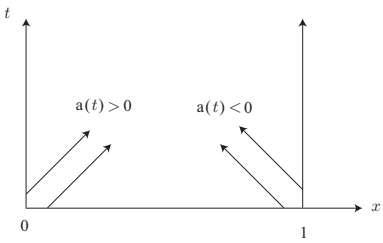

Fig. 1. a(t) conditions for the PDE stability

(dissolution phase). The stability of the equation system during the dissolution phase permits the estimation of the remaining part. The PDE describing the metastable CSD is an hyperbolic equation, it has the following form :

$$\frac{\partial F(x,t)}{\partial t} + a(t)\frac{\partial F(x,t)}{\partial x} = 0 \qquad (22)$$

Figure (1) gives the condition for the stability of the equation (22), the variable x is normalized ($0 \leq x \leq 1$). The stability is guaranteed if the condition concerning $a(x)$ is respected. In our case, when the metastable form is in dissolution phase, $G_2(t)$ is replaced by $D_2(t)$, this dissolution kinetic gives negative values, thus, the system is stable, which allows the boundedness of the error between the model and the estimated values.

3. DISCRETIZATION OF THE PBE "POPULATION BALANCE EQUATION"

Finite difference method is applied in the current study for the discretization of the PBEs. This choice is motivated by the structure obtained by this method which corresponds exactly to the observer one. Indeed, the state matrix involved exhibits tri-diagonal form. Moreover, the method concurs with the physical behavior of the system. The principle of the discretization for (1) and (2) is exactly the same. The system resulting for one of the two PDEs from the discretization turns out to be :

$$\begin{cases} \dot{n_x} = \alpha(t)An_x \\ y = Cn_x \end{cases} \qquad (23)$$

With:

$$\alpha(t) = \frac{G(t)}{\Delta x} \qquad (24)$$

In the case of dissolution :

$$\alpha(t) = \frac{D(t)}{\Delta x} \qquad (25)$$

$$n_x = \begin{pmatrix} n_{x_1} \\ n_{x_2} \\ n_{x_3} \\ \vdots \\ n_{x_{N-1}} \\ n_{x_N} \end{pmatrix}, A = \begin{pmatrix} 1 & -1 & 0 & \dots & 0 \\ \frac{1}{2} & 0 & -\frac{1}{2} & \ddots & \vdots \\ 0 & \ddots & \ddots & \ddots & 0 \\ \vdots & \ddots & \frac{1}{2} & 0 & -\frac{1}{2} \\ 0 & \dots & 0 & 0 & 0 \end{pmatrix}, C = \begin{pmatrix} 1 & 0 & \dots & \dots & 0 \end{pmatrix},$$

Where $n_x \in \mathbb{R}^N$, $A \in \mathbb{R}^N \times \mathbb{R}^N$ and $C \in \mathbb{R}^N$

4. HIGH GAIN OBSERVER SYNTHESIS

As far as the crystal forms are supersaturated, system (23) associated to the output $\frac{Rn(t)}{G(t)}$ is observable. The production of nuclei allows to synthesize a high gain observer. In the undersaturation case, measurements are not available. However, an open loop observer may be applied to both forms to estimate the CSDs. The convergence of the proposed observer is dependent on the stability of the PBEs. In the following, the observer is applied for both PBEs. In the case of single output systems, the high gain observer is dedicated to the uniformly observable systems class of the following form :

$$\begin{cases} \dot{z} = f(z) + \sum_{i=1}^{N} u_i g_i(z) \\ y = h(z) \end{cases} \quad (26)$$

where $z(t) \in \mathbb{R}^N, y \in \mathbb{R}, u \in \mathbb{R}^p$ System (26) is said to be uniformly observable if for any two initial states $z \neq \bar{z}$ and every admissible inputs defined on any $[0, T]$, there exists $t \in [0, T]$ such that $y(z, u, t) \neq \bar{y}(\bar{z}, u, t)$, where y(z,u,t) is the output associated to the initial state z and the input u. In our case, system(26) takes the particular form of system (23) which is clearly observable due to its triangular form. The canonical form may be used to construct an exponential observer for system (23) under the following assumption :
$0 < \gamma \leq \alpha(t) \leq \xi \ \forall t \geq 0$
for some constants γ and ξ.
With continuous measurements, a candidate exponential observer for this system is given by (Farza *et al.*, 1997) and (Gauthier *et al.*, 1992):

$$\dot{\hat{z}}(t) = \alpha(t) A \hat{z}(t) - \alpha(t) S_\theta^{-1} C^T (C\hat{z}(t) - Y(t)), \quad (27)$$

where S is symmetric positive definite matrix given by the following equation :

$$\dot{S}_\theta(t) = -\theta S_\theta(t) - A^T S_\theta(t) - S_\theta(t) A + C^T C \quad (28)$$

If $\alpha(t)$ is negative for any time $t > 0$, the sign of the correction term should be changed :

$$\begin{cases} \dot{\hat{z}}(t) = \alpha(t) A(t) \hat{z}(t) + \\ \qquad \alpha(t) S_\theta^{-1} C^T (C\hat{z}(t) - Y(t)) \end{cases} \quad (29)$$

An other alternative is to use the following diffeomorphism $\phi : \mathbb{R}^N \to \mathbb{R}^N$
$z \to \phi(z) = [h, L_f(h), \dots, L_f^{n-1}(h)]$
Such diffeomorphism transforms the system (23) into the observable canonical form with :

$$A_1 = \begin{pmatrix} 0 & 1 & \dots & 0 \\ 0 & 0 & \ddots & \vdots \\ \vdots & \vdots & \ddots & 1 \\ 0 & 0 & \cdots & 0 \end{pmatrix}, C_2 = \begin{pmatrix} 1 & 0 & \dots & 0 \end{pmatrix},$$

The resulting observer has the following form :

$$\dot{\hat{z}}(t) = \alpha(t) A \hat{z} - \alpha(t) (\frac{\partial \phi}{\partial z}(\hat{z}, t))^{-1} S_\theta^{-1} C_2^T (C_2 \hat{x}(t) - Y(t)) \quad (30)$$

Where S_θ is given by the following Lyapunov equation :

$$\theta S_\theta(t) + A^T S_\theta(t) + S_\theta(t) A = C^T C \quad (31)$$

The terms of this matrix $S_\theta = [S_\theta(l,k)]_{1 \leq l,k \leq N}$ have the following form :

$$S_\theta(l,k) = \frac{(-1)^{l+k} D_{l+k-2}^{k-l}}{\theta^{l+k-1}} \quad (32)$$

With :

$$D_n^k = \frac{n!}{(n-k)!k!} \quad (33)$$

5. SIMULATION RESULTS AND DISCUSSION

5.1 Simulation conditions

The parameters used in this simulation are taken from the crystallization of adipic acid in water by (Marchal, 1989). Predictive models of homogenous primary nucleation A_1 were also taken from (Mersmann *et al.*, 2000). Concerning the jacket, the cooling fluid is assumed to be brine at $0°C$. Figure 2 summarizes the parameters values which were used during the simulation.

5.2 Simulation discussion

Figure (3) represents the solute concentration profile and the saturation concentration for both crystal forms. It can be seen that between the two temperatures (322K and 312K), the nuclei production of both forms is very small. For lower temperature, nucleation and crystal growth begin and stay until a temperature of about 300K. Below 300K, the metastable form is undersaturated while the stable form is supersatured. The metastable form therefore begins to dissolve. Nucleation and growth of the stable form still go on.

Figures (4) and (5)represent some examples of simulated classes of crystal sizes and the corresponding estimated ones. The choice of these crystal sizes is arbitrary. The same performances can

parameter	definition	unit	value
A_{11}	homogeneous primary nucleation parameter for CSD 1	$nb.m^{-3}.s^{-1}$	1 10^{10}
B_{11}	homogeneous primary nucleation parameter for CSD 1	$nb.m^{-3}.s^{-1}$	0.63
A_{21}	homogeneous primary nucleation parameter for CSD 2	$nb.m^{-3}.s^{-1}$	1 10^{12}
B_{21}	homogeneous primary nucleation parameter for CSD 2	$nb.m^{-3}.s^{-1}$	0.63
A_{12}	secondary nucleation parameter for CSD 1	$nb.m^{3(i+j-1)}mol^{-i-j}.s^{-1}$	1440
K_{c1}	growth constant for CSD 1	$mol^{(1-g)}.m^{(3g-2)}.s^{-1}$	0.0157
A_{22}	secondary nucleation parameter for CSD 2	$nb.m^{3(i+j-1)}mol^{-i-j}.s^{-1}$	1440
K_{c2}	growth constant for CSD 2	$mol^{(1-g)}.m^{(3g-2)}.s^{-1}$	0.0170
K_{dis1}	growth constant for CSD 1	$mol^{(1-g)}.m^{(3g-2)}.s^{-1}$	2 10^{-8}
K_{dis2}	growth constant for CSD 2	$mol^{(1-g)}.m^{(3g-2)}.s^{-1}$	2.5 10^{-8}
i	exponent	no dimension	1.968
j	exponent	no dimension	1
g	exponent	no dimension	2
M_s	molar mass	$Kg.mol^{-1}$	146.14 10^{-3}
ρ_s	volume mass	$Kg.m^{-3}$	1360
K_{V1}	shape factor for CSD 1	no dimension	$\frac{\pi}{6}$
K_{V2}	shape factor for CSD 2	no dimension	$\frac{\pi}{10}$
Cp_1	solute molar heat capacity	$J.K^{-1}.mol^{-1}$	3.72
Cp_2	solid molar heat capacity	$J.K^{-1}.mol^{-1}$	7.44
Cp_1	water molar heat capacity	$J.K^{-1}.mol^{-1}$	75.33
ΔH_c	crystallization enthalpy	$J.mol^{-1}$	-48000
U	overall heat transfer coefficient	$J.m^{-2}.K^{-1}.s^{-1}$	1000
A_c	contact surface through jacket wall	m^2	0.022

Fig. 2. simulation parameters values

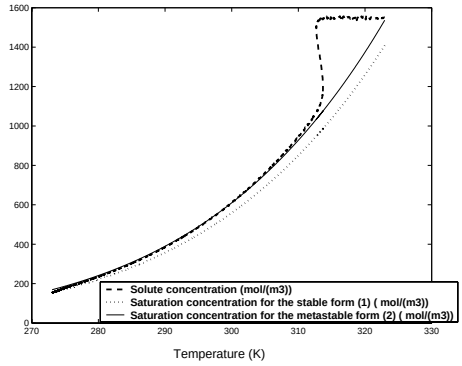

Fig. 3. solubility for stable and metastable forms

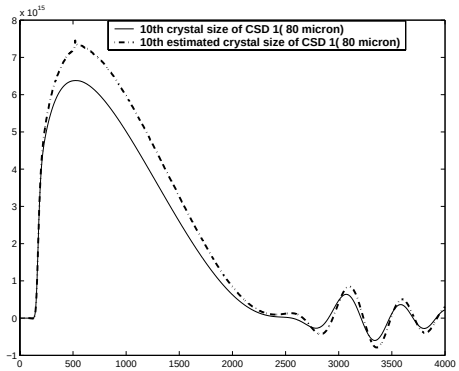

Fig. 4. 1Oth size crystal of the stable form (Model and estimate (dotted))

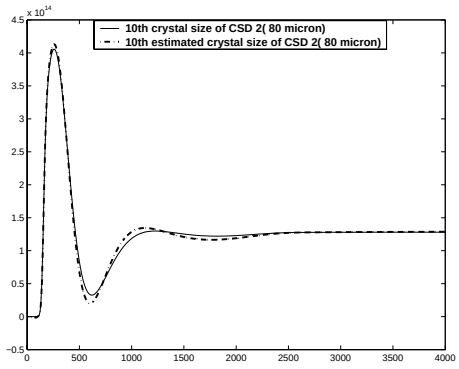

Fig. 5. 1Oth size crystal of the metastable form (Model and estimate (dotted))

be shown for the other sizes. Figure (4) represents the time variation of the number of stable crystals in the 10th size class (i.e. size around 80 μ m) and its estimation. Figure (5) represents the crystal size of the metastable form and its estimation. Before 500 s, the metastable form is supersaturated. Then, the metastable form becomes undersaturated (this time corresponds to the temperature of 300K), the open loop observer is then used. As mentioned above, the stability of the system yield by the PBE discretization implies the assymptotic convergence of the observer. The crystal size and its estimate tend to the same final value with an acceptable error, as shown on the figure.

Figures (6) and (7) represent the CSD of the stable form and its estimation. Figures (8) and (9) represent the CSD of metastable form and its es-

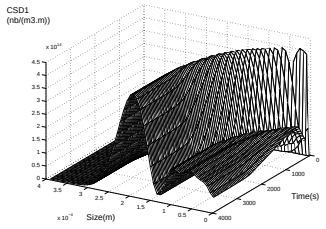

Fig. 6. crystal size distribution based on stable form model

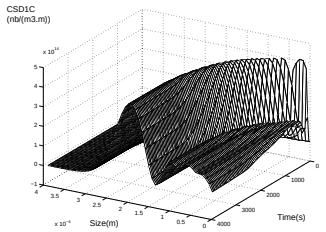

Fig. 7. estimation of stable form crystal size distribution

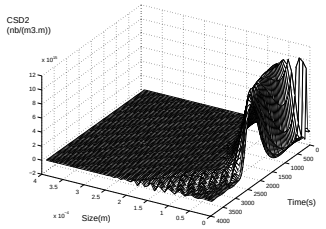

Fig. 8. crystal size distribution based on metastable form model

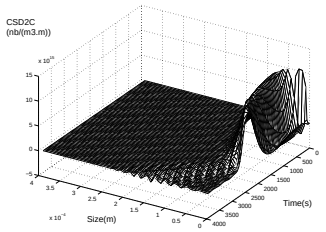

Fig. 9. estimation of metastable form crystal size distribution

timation. These figures summarize the comments made after the preceding results. The estimation of both CSD's is acceptable.

6. CONCLUSION

In this work, a methodology to estimate CSDs in polymorphic crystallization process has been presented. This methodology is based on a model for each crystal form. This model in obtained by the solute concentration balance, the energy balance in the crystallizer in addition to population balance equations for both crystal forms. A high gain observer is applied to estimate the CSDs of stable and metastable forms in nucleation phase. In the dissolution phase, the metastable form can be estimated using open loop estimation. This estimation gives good results because of the stability of the PBEs. Additional simulations have shown that modelling errors in primary nucleation parameters don't affect considerably the observer robustness.The observer can be used for process supervision to prevent any variation of crystals population which may affect the product quality. In the case of control applications, the estimated crystal size distribution could be used to ensure advanced quality control objectives such as reproducible crystal number mean sizes and variances.

REFERENCES

Caillet, A., F. Puel and G. Fevotte (2006). In-line monitoring of partial and overall solid concentration during solvent-mediated phase transition using raman spectroscopy. *International journal of pharmaceutics* **307(2)**, 201–208.

Farza, M., H. Hammouri, S. Othman and K. Busawon (1997). Non linear observer for parameter estimation in bioprocesses. *Chemical engeneering Science* **52**, 4251–4267.

Gauthier, J.P., H. Hammouri and S. Othman (1992). A simple observer for non linear systems application to bioreactors. *IEEE Trans. Automat. Control* **37**, 875–880.

Marchal, P. (1989). *Génie de la cristallisation: application l'acide adipique*. Thesis,Institut National Polytechnique de Lorraine. Nancy.

Mersmann, A., B. Braun and M. Löfflmann (2000). Prediction of crystallization coefficients of the population balance. *Chemical engeneering science* **57**, 4267–4275.

Ono, T., H. J. M. Kramer, J. H. ter Horst and P. J. Jansens (2004). Process modeling of the polymorphic transformation of l-glutamic acid. *Crystal growth and design* **4**, 1161–1167.

Starbuck, C., A. Lindemann, L. Wai, J. Wang, P. Fernandez, C. Lindemann, G. Zhou and Z. Ge (2002). Process optimization of a complex pharmaceutical polymorphic system via in situ raman spectroscopy. *Crystal growth and design* **2**, 515–522.